Forecasting the Propagation of HF Radio Waves Over Bulgaria

Rumiana Bojilova and Plamen Mukhtarov

Abstract A new methodology for forecasting the propagation of HF radio waves by reflection from the ionosphere over Bulgaria in the absence of ionosonde data is presented. The proposed methodology contains three main parts. Based on the long-term ionosonde data an empirical model of the critical E region frequency (*foE*) has been built; the latter depends on the season, local time and the level of solar activity described by the solar radio flux at 10.7 cm wavelength (*F10.7*). The critical frequency of the F2-layer (*foF2*) and the maximum usable frequency at a propagation of 3000 km (*MUF3000*) are obtained by means of the proposed empirical relationships between these two critical frequencies and the Total Electron Content (*TEC*). Based on these three ionospheric characteristics a modeled electron density profile is compiled by using the method of Di Giovani-Radicella (Giovanni and Radicella in Adv Space Res 10:27–30, 1990 [1]). The constructed in this way electron density profile allows calculating the lowest and maximum usable frequency at a given distance up to 500 km according to the theory of radio wave propagation in the ionospheric plasma, namely the equivalence theorem and the secant law, as well as the law of reduction of the group velocity of propagation depending on the ionosphere electron density.

Keywords HF radio waves · Electron density profile · Empirical model

1 Introduction

Radio communication and broadcasting systems can be divided into either controlled by the ionosphere, as in HF sky-wave systems, or simply affected by it, as in trans-ionospheric radio signals, used by the Global Navigation Satellite Systems (GNSS) for communication and navigation systems. In the former case, the ionosphere is actually an inflexible part of the system; while in the latter case, the ionosphere is the largest source of errors, i.e. errors in GNSS positioning, timing and navigation. In

R. Bojilova (✉) · P. Mukhtarov
National Institute of Geophysics, Geodesy and Geography, Bulgarian Academy of Sciences (NIGGG-BAS), Acad. Georgi Bonchev str., Bl. 3, 1113 Sofia, Bulgaria
e-mail: rbojilova@geophys.bas.bg

N. Dobrinkova and G. Gadzhev (eds.), *Environmental Protection and Disaster Risks*, Studies in Systems, Decision and Control 361,
https://doi.org/10.1007/978-3-030-70190-1_21

both instances however, an account of the ionosphere is at least beneficial to system design and operation [2]. The present study is directed to the first case systems and particularly for not very long-range ones because mainly the propagation of HF radio waves (HF is usually taken as the frequency band of 2–30 MHz) by reflection from the ionosphere over Bulgaria will be considered.

The basic aim of the radio wave propagation forecasting is to improve communication systems and give recommendation about the future reliability of frequency bands propagated via the ionosphere. The impact of the ionosphere on the radio wave propagation has been well known since the past several decades and is described by the relationship between plasma frequency and signals which propagate within that medium. A wide range of telecommunication systems have been developed and many have been fielded for operational use. While many of the systems received their impetus through military necessity, the utility of telecommunications is evident in virtually all aspects of human activity [3]. In civilian society the HF communication is used predominantly by radio amateurs and for international broadcasts by different government organizations. The use of HF communication is preferred due to its relative simplicity, its capability to provide long range communication at low power without repeater base stations, its ease of development and its low cost. The disadvantage is low throughput of HF channel and significant influence of propagation environment (ionosphere variability) on the quality of transmission.

It is known that to provide accurate prediction method of HF radio systems different ionospheric models are needed. The models considered are for the ionospheric characteristics and electron density profile models, a propagation model, transmission loss and characteristics of the radio noise models [4]. This means that for producing different ionospheric models, particularly over a limited region, long-term ionosonde measurements of the main ionospheric characteristics over the considered region have to be available. The basic aim of the present study is to offer a new methodology for forecasting the propagation of HF radio waves by reflection from the ionosphere over Bulgaria in the absence of data from a vertical sounding station.

2 Empirical Model for FoE Prediction

This study uses the data from vertical sounding of the ionosphere from the ionosonde station Sofia at the National Institute of Geophysics, Geodesy and Geography, Bulgarian Academy of Sciences for the period of 1995–2014, as well as the data for solar and geomagnetic activity from the National Oceanic and Atmospheric Administration, USA.

The basis of the model idea for *foE* prediction is connected with the stable dependence of the E-region maximum electron density in day time conditions

$$N_{mE}\left[\mathrm{cm}^{-1}\right] = 1.24.10^4 foE^2[\mathrm{MHz}] \tag{1}$$

from the cosine of the solar zenith angle, which is due to the fact that the electron density in the E region with sufficient accuracy obeys Chapman's theory [5]. Figure 1 shows the dependence of the monthly medians of the maximum electron density NmE on the solar zenith angle cosχ for four years: high solar activity in 1999, declining phase in 2003, low solar activity in 2008 and rising phase in 2011. The wanted dependence with sufficient accuracy is represented by a second degree polynomial calculated by a least squares method and shown by solid line in the plots. It is obvious that this dependence is different in the presented four years which is due to the solar cycle impact on the ionizing radiation. Pancheva and Mukhtarov [6] demonstrated that the dependence of N_{mE} on the solar zenith angle varies not only on the solar activity, but also the season and is different before local noon compared to that after noon.

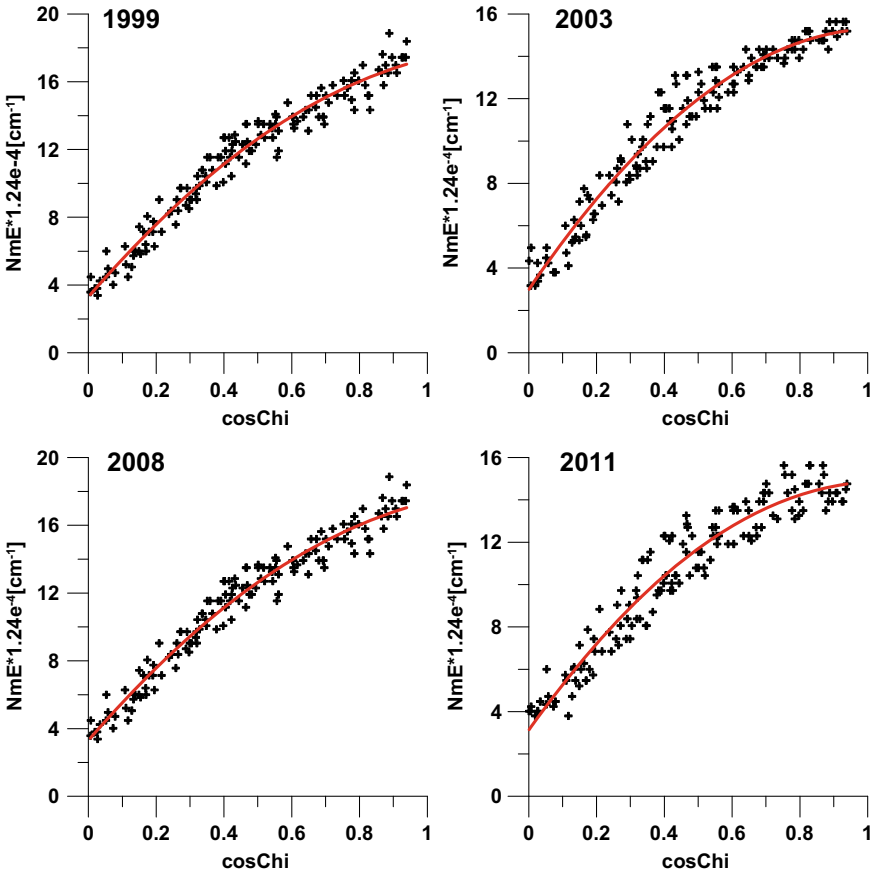

Fig. 1 Solar zenith dependence of the critical frequency *foE* during different solar activity conditions; 1999 (upper left plot) shows high solar activity; 2003 (upper right plot) declining phase; 2008 (bottom left plot) low solar activity, and 2011 (bottom right plot) rising phase

The most ionospheric modelers use the sunspot number (number of dark spots on the solar disc) and the solar radio flux at 10.7 cm wavelength (*F10.7*) as solar indices, since both can be observed from the ground, long data records exist and they can be predicted. These indices together with their 6-month predictions are regularly published by [7]. Some preliminary experiments were performed with both indices and the results revealed that particularly for the considered last solar cycle *F10.7* describes better the ionospheric variability. Thus, in the present study *F10.7* is used as a proxy for the solar activity. It is known however that the ionosphere behaves differently at the rising and declining phase of the solar cycle at one and the same *F10.7* [8–10]. To include this ionospheric feature in the model an additional parameter *kF10.7* is used which describes the linear rate of change of *F10.7*. The idea for describing the solar activity by such two parameters, i.e. by the level of solar activity and its tendency, was introduced for the first time by [11] in modeling the monthly median critical frequency of the ionospheric F-region, *foF2*, above Sofia. It was found that the inclusion of the *kF10.7* in the monthly median *foF2* model decreased its mean standard deviation by ~0.5 MHz. Later this idea was successfully applied in building of global background *TEC* model reported by [12]. In this study the smoothed time series of *F10.7* is used obtained by a sliding 11-month window and denoted as *sF10.7*.

Usually the seasonal dependence the electron density in the E region is described only by both annual and semiannual components. In this study however the seasonal components with periods shorter than 6 months have also some contribution even though they are weaker than annual and semiannual ones.

Based on the above mentioned clarifications the empirical model of the maximum electron density N_{mE} separately for for-noon N_{mEfn} and afternoon N_{mEan} conditions can be described by the following functions:

$$\begin{aligned}
&N_{mEfn}(sF10.7, kF10.7, \text{month}, \cos\chi)\\
&= \left(a_{0fn} + a_{1fn}sF10.7 + a_{2fn}sF10.7^2 + a_{3fn}kF10.7 + a_{4fn}kF10.7^2 + a_{5fn}sF10.7kF10.7\right)\\
&\quad\times\left(b_{0fn} + \sum_{k=1}^{4} b_{1kfn}\cos\left(k\frac{2\pi}{12}\text{month}\right) + b_{2kfn}\sin\left(k\frac{2\pi}{12}\text{month}\right)\right)\\
&\quad\times\left(c_{0fn} + c_{1fn}\cos\chi + c_{2fn}\cos\chi^2\right) \qquad (2)\\
&N_{mEan}(sF10.7, kF10.7, \text{month}, \cos\chi)\\
&= \left(a_{0an} + a_{1an}sF10.7 + a_{2an}sF10.7^2 + a_{3an}kF10.7 + a_{4an}kF10.7^2 + a_{5an}sF10.7kF10.7\right)\\
&\quad\times\left(b_{0an} + \sum_{k=1}^{4} b_{1kan}\cos\left(k\frac{2\pi}{12}\text{month}\right) + b_{2kan}\sin\left(k\frac{2\pi}{12}\text{month}\right)\right)\\
&\quad\times\left(c_{0an} + c_{1an}\cos\chi + c_{2an}\cos\chi^2\right) \qquad (3)
\end{aligned}$$

The expression in the first right hand bracket of the above formulas (2) and (3), i.e. the Taylor series expansion up to degree of 2, represents the solar activity term which modulates the seasonal and day time behavior of the ionosphere. The seasonal

term (expression in the second right hand bracket) includes 4 sub-harmonics of the year, i.e. annual, semiannual, 4- and 3-month components; it modulates the day time behavior of the ionosphere. The expression in the last, third right hand bracket is again a Taylor series expansion up to degree of 2, describing the solar zenith angle day time variability of the E-region shown in Fig. 1.

The empirical *foE* model described by (2) and (3) contains 162 constants and they are determined by the least squares fitting techniques, i.e. at minimizing the root mean square error of the model relative to the data.

Figure 2 presents the comparisons between the model *foE* results (thin line with dots) and the observations (thick line) for two years with different solar activity; 2000 for high solar activity (upper plot) and 2007 for low solar activity (bottom plot). The root mean square error (*RMSE*) calculated for the whole data set is 0.083 MHz, i.e. this is a completely satisfactory result.

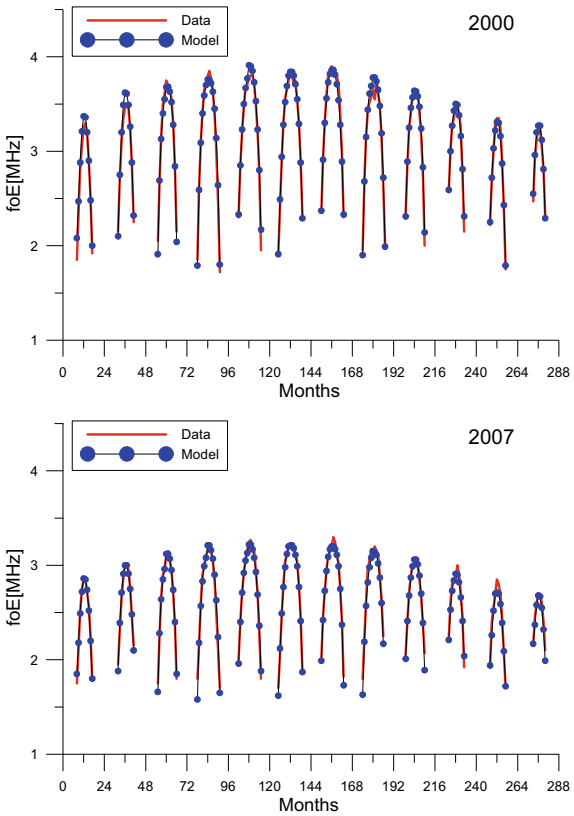

Fig. 2 Comparison between the model data (thin line with dots) and observations (thick line) for 2000 (upper plot, high solar activity) and 2007 (bottom plot, low solar activity)

3 Empirical Model for Calculating FoF2 and MUF3000 Based on TEC Data

The reason for building such a model is the fact that the main part of the TEC is formed by the region of the electron density profile around the maximum of the F region and it is reasonable to expect a well-defined relationship between the maximum electron density $N_{mF2}[\mathrm{cm}^{-1}] = 1.24\ 10^4\ (foF2[\mathrm{MHz}])^2$ and the *TEC* [13].

The regressions shown in Figs. 3 and 4 indicated that the wanted dependence between foF2 or MUF3000 on TEC can be described as a second degree polynomial.

$$\begin{aligned} foF2 &\approx a_f(\text{month}, UT)TEC^2 \\ &\quad + b_f(\text{month}, UT)TEC + c_f(\text{month}, UT); \\ MUF3000 &\approx a_m(\text{month}, UT)TEC^2 \\ &\quad + b_m(\text{month}, UT)TEC + c_m(\text{month}, UT) \end{aligned} \tag{4}$$

The constants of the above models are determined by least squares fitting techniques based on the *foF2* and *MUF3000* data from the ionosonde station Sofia and TEC data from the Center for Orbit Determination of Europe (CODE) for the closest to Sofia point (42.5° N, 25° E) for the period of 1999–2014.

The comparison between the model and measured *foF2* and *MUF3000* values reveals that the mean error is practically zero while the *RMSE* for *foF2* is e 0.55 MHz and for *MUF3000* is 2.1 MHz. For practical purposes this error can be considered as permissible. Further, a mathematical procedure for obtaining *foF2* and *MUF3000* values from vertical *TEC* measurements has been proposed very recently by [14]. The mathematical relationships between F2-layer characteristics and vertical TEC values have been derived using South-African co-located ionosonde and GNSS stations but the same procedure can be applied successfully in each region where such data are simultaneously available. Evaluating the error of this transformation the authors found *RMSE* for *foF2* to be 0.754 MHz, while for *MUF3000* is 2.782 MHz; hence both errors are larger than the obtained ones in this study.

Figure 5 presents the comparison between the measured (red line) and reconstructed by *TEC* (blue line) ionospheric characteristics *foF2* (left panel) and *MUF3000* (right panel) for the period of time 21–31 October 2003. The considered time interval was selected due to the registered extremely strong geomagnetic storms, known as Halloween geomagnetic storms, in the period of 29–30 October 2003. It can be seen from Fig. 5 that the coincidence between the measured and modeled values is satisfactory not only in the quiet days of the month but also in the disturbed ones. The mean *foF2* error for the considered time interval is 0.2 MHz while that for *MUF3000* is 1.55 MHz; the corresponding *RMSE* for *foF2* is 0.73 MHz and for *MUF3000* is 3.47 MHz. The *RMSE* values of the two ionospheric parameters in the above discussed example do not differ significantly from the errors for whole interval of years (1999–2014).

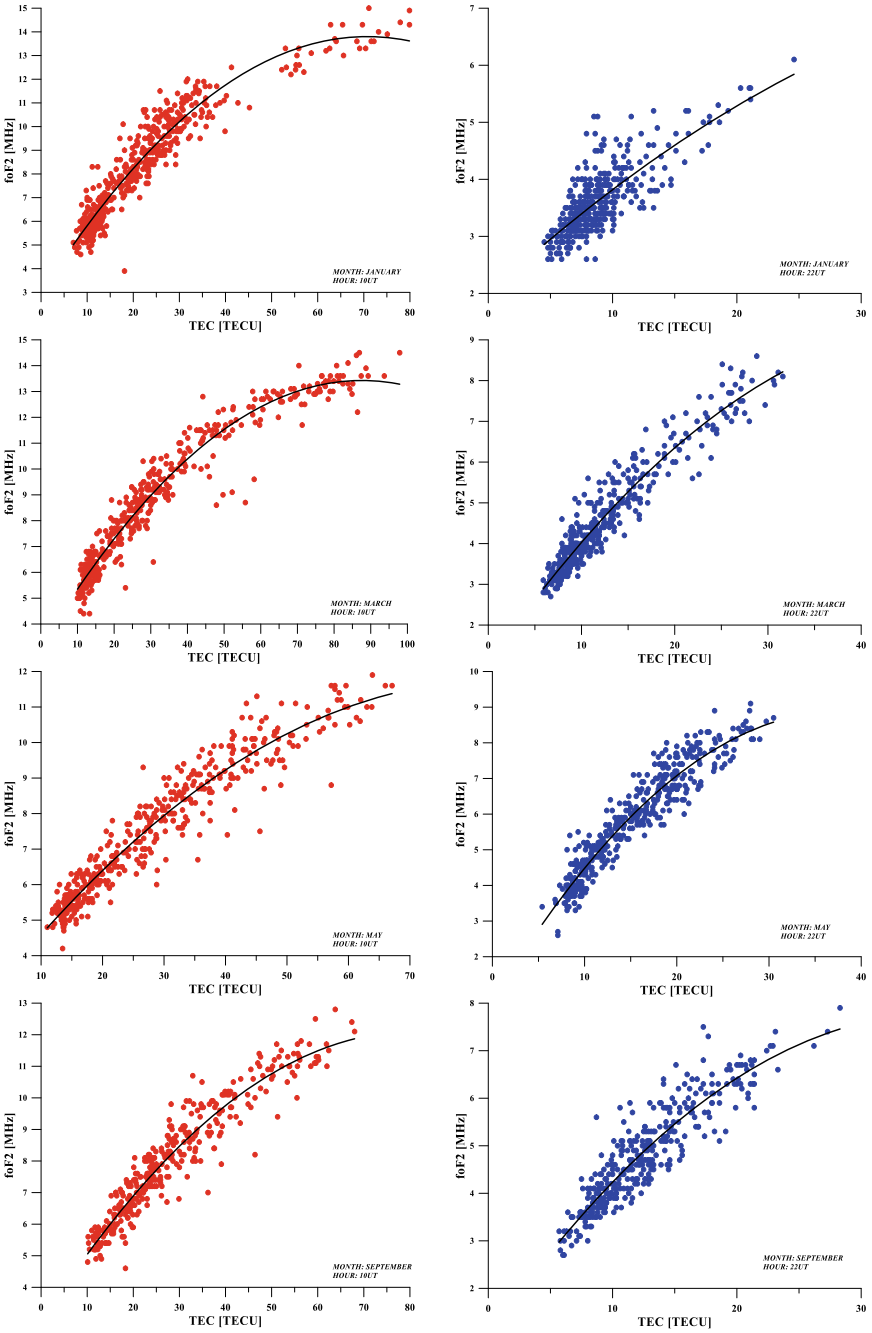

Fig. 3 Regression dependences of *foF2* on *TEC* for the calendar months January, March, May and September for 10 UT (left column panels) and 22 UT (right column panels) obtained from all data (1999–2014)

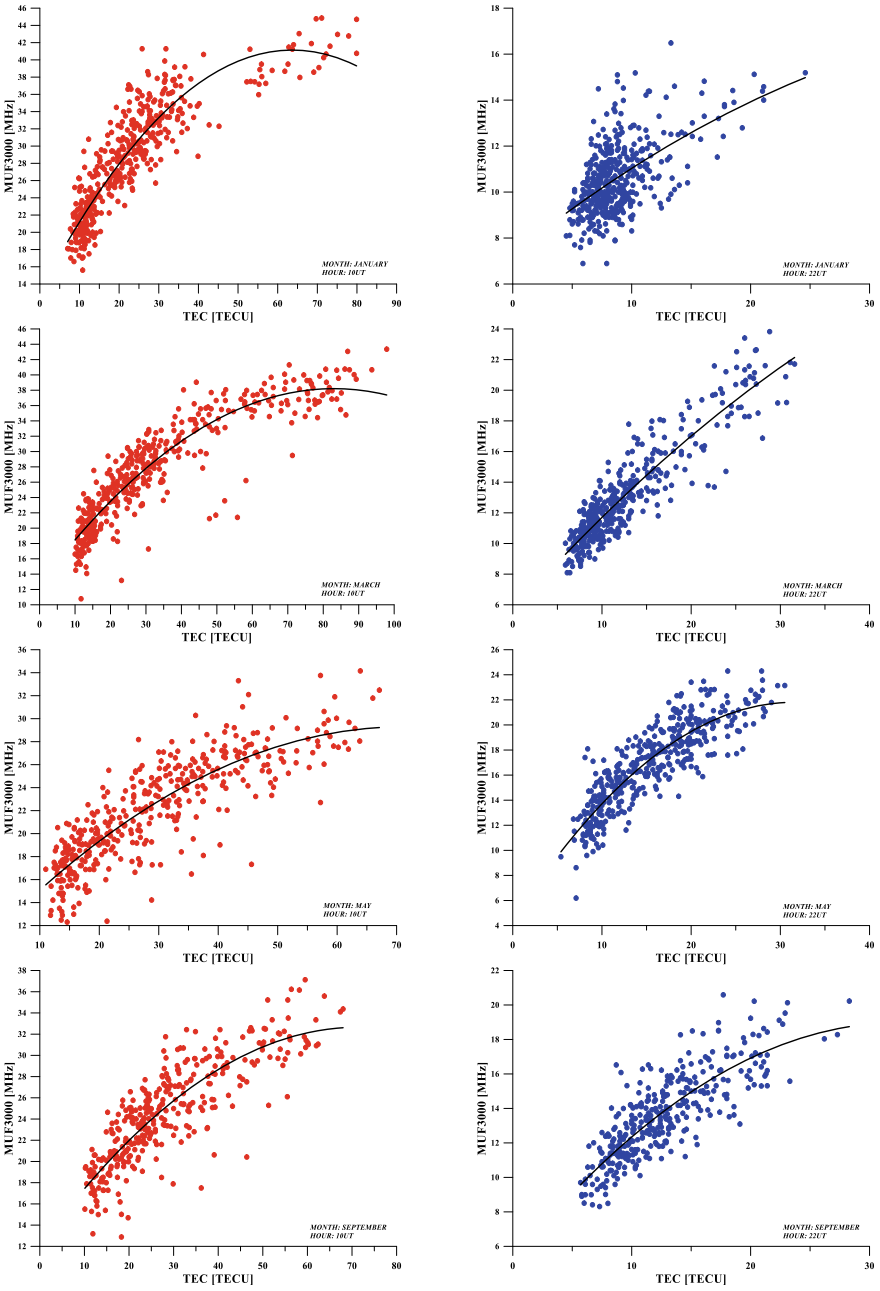

Fig. 4 The same as Fig. 3 but for regression dependences of *MUF3000* on *TEC*

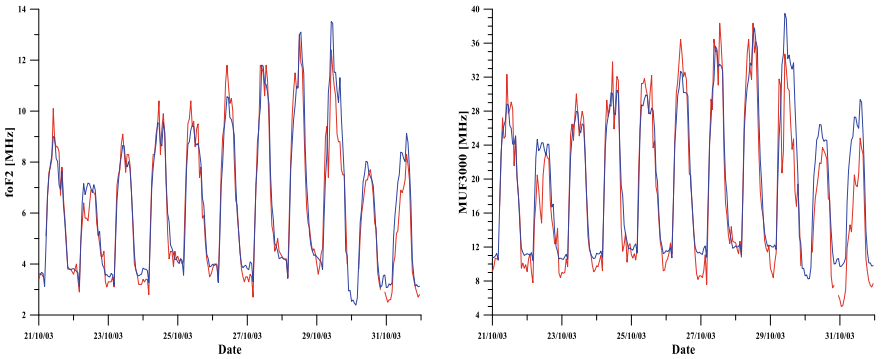

Fig. 5 (left panel) Comparison between the reconstructed by *TEC* hourly values of *foF2* (blue line) and the measured ones (red line) for the period of 21–31 October 2003; (right panel) the same as the left panel but for *MUF3000*

The use of the data from CODE for producing an empirical model for the *foF2* prediction based on the *TEC* data is caused by the available long enough time period when there simultaneous ionosonde and *TEC* data. However, the data from CODE arrive with a delay of one day. We note that there is a possibility to use data arriving in a real time from a single GNSS receiver operating in the territory of Sofia, denoted as station SOFI. The methodology for calculating the vertical *TEC* from the raw data has been reported by [15].

4 Model Electron Density Profile for a Given Time

After defining the critical frequencies based on the above described methodology, the construction of the electron density profile has been performed according to [1].

For day-time conditions:

$$h \le h_{mE};$$

$$N(h) = N_{mE}\,\mathrm{sech}^2\left(\frac{h_{mE} - h}{2B_{Eb}}\right)$$

$$h > h_{mE};$$

$$N(h) = \left(N_{mE} - N_{mF}\,\mathrm{sech}^2\left(\frac{h_{mF2} - h_{mE}}{2B_F}\right)\right)\mathrm{sech}^2\left(\frac{h - h_{mE}}{B_{Et}}\right) + \left(N_{mF2} - N_{mE}\,\mathrm{sech}^2\left(\frac{h_{mF2} - h_{mE}}{2B_{Et}}\right)\right)\mathrm{sech}^2\left(\frac{h - h_{mF2}}{B_F}\right) \quad (5)$$

and respectively for night-time conditions:

$$f_{oE} = 0;$$
$$N(h) = N_{mF2}\text{sech}^2\left(\frac{h_{mF2} - h}{B_f}\right) \tag{6}$$

This model is based on the representation of the electron density profile with hyperbolic secant functions [13].

The values of the three critical frequencies are sufficient to calculate the model electron density profile for heights up to the height of the F-region maximum; the latter is calculated by the given below formulas. The maximum electron concentration of both the E and F layers are determined directly by the critical frequencies.

The height of the E-layer maximum is assumed to be fixed 120 km. The model uses the empirically determined by [16] dependence of the height of the F2-layer maximum h_{mF2} on the parameter $M3000F2 = MUF3000F2/foF2$, the ratio $foF2/foE$ and the correction value D_m according to the given below formulas. The parameter B_f, related to the half-thickness of the ionospheric F-layer, is expressed by an empirical dependence of the derivative of the electron profile dN/dh, which in turn is expressed by the values of $foF2$ and $M3000F2$. The half-thicknesses of the E-layer (B_{Eb}-below and B_{Et}-above the maximum of the E-region) take fixed values.

$$N_{mE}\left[\text{cm}^{-2}\right] = 1.24.10^4 foE^2[\text{MHz}]$$
$$N_{mF2}\left[\text{cm}^{-2}\right] = 1.24.10^4 foF2^2[\text{MHz}]$$

$$h_{mE} = 120\,\text{km};\ \ B_{Eb} = 7.5\,\text{km};\ \ B_{Et} = 7\,\text{km} \tag{7}$$

$$h_{mF2} = 1470\frac{M_f}{M3000F2 + D_m} - 176$$

$$M3000F2 = \frac{MUF3000}{foF2}$$

$$B_f = 0.04774.10^{11}\frac{foF2^2}{dN/dh}$$

$$M_f = M3000F2\sqrt{\frac{0.0196M3000F2^2 + 1}{1.2967M3000F2^2 - 1}} \tag{8}$$

$$dN/dh = 1.10^9\exp\left(-3.467 + 0.857\lg\left(foF2^2\right) + 2.02\lg(M3000F2)\right)$$

5 Calculation of the Radio-Path Parameters

The task for the calculation of radio paths contains the determination of the frequency range at which a radio communication at a given distance between the two radio communication points can take place. The frequency range is limited by the lowest and maximum usable frequencies (*LUF* and *MUF* respectively), which depend on the distance of the radio communication and the state of the ionosphere at the respective time.

The calculation methodology is based on the theory of radio wave propagation without taking into account the influence of Earth's magnetic field. We note that this simplification does not reduce the accuracy of the calculation. Upon entering the ionosphere, radio waves suffer the so-called magnetic-ion splitting, i.e. they break up into two separate waves that propagate at different speeds. Traditionally, the data from the ionograms take into account ionospheric characteristics (e.g. critical frequencies) of the reflections of the ordinary wave. The propagation of an ordinary wave is not affected by the presence of the Earth's magnetic field [17, 18].

The geometry of the ionospheric reflection is illustrated schematically in Fig. 6. In the case of vertical radio-wave propagation, the virtual reflection height of the ordinary wave h'_{vert} depending on the frequency f is obtained according to the formula (9) below.

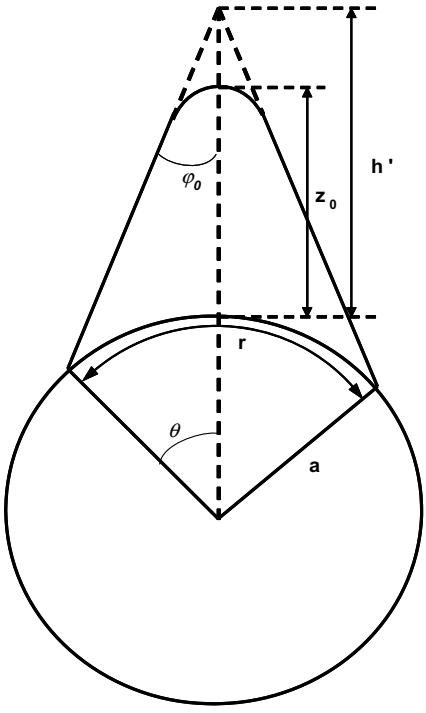

Fig. 6 Basic geometrical ratios at oblique reflection of radio signals from the ionosphere

$$h'_{vert}(f) = \int_0^{z_0} \frac{dz}{\sqrt{1 - 80.8\frac{N(z)}{f^2}}}$$
$$80.8\frac{N(z_0)}{f^2} = 1 \tag{9}$$

where $N(z)$ is the altitude electron density profile. The height z_0 is that height at which the denominator of the sub-integral function is canceled, which means the so-called "full internal reflection" when the radio wave changes its direction of propagation. When the electron density profile has a maximum at altitude of z_0 then the integral tends to infinity for the corresponding frequency.

The ratio between the frequencies and virtual heights in the cases of vertical and oblique propagation is given by the equivalence theorem and the secant low:

$$h'_{ob}(f_{ob}) = h'_{vert}(f_{vert}) \sec \phi_0$$
$$f_{ob} = f_{vert} \sec \phi_0 \tag{10}$$

The secant theorem shown in the formula reflects the following regularity. An oblique ray with a frequency f_{ob} incident on the ionosphere at an angle φ_0 is reflected by the ionosphere at the same height as a vertical ray with a frequency f_{vert}.

Based on Fig. 6 it follows:

$$tg\phi_0 = \frac{a\sin(\theta)}{h'_{vert} + a(1 + \cos(\theta))} \tag{11}$$

where a is the radius of the Earth (about 6370 km), the angle θ is half of the central angle between the two endpoints of the radio path. If the length of the radio path on the Earth's surface is denoted by r, then its angle θ in radians can be calculated by:

$$\theta[\text{rad}] = \frac{r}{2a} \tag{12}$$

The calculation of a given radio-path begins with calculating the model ionogram $h'_{vert}(f_{vert})$ by numerical integration of the model electron density profile. The left panel of Fig. 6 shows examples of electron density profiles at noon (solid line) and midnight (dash line) conditions (electron density is expressed in plasma frequencies) while the right panel presents the corresponding model vertical ionograms.

After calculating the model vertical ionograms, the reflection frequencies of the respective virtual heights at oblique propagation are determined according to the secant theorem. As a result the so-called "oblique ionogram" $h'_{ob}(f_{ob})$ dependence at a given distance of the radio-path is found. Figure 8 shows the oblique ionograms for three distances based on the electron density profiles presented in the left panel of Fig. 7; the midnight ionograms can be seen in the left panel while the noon time ones in the right panel.

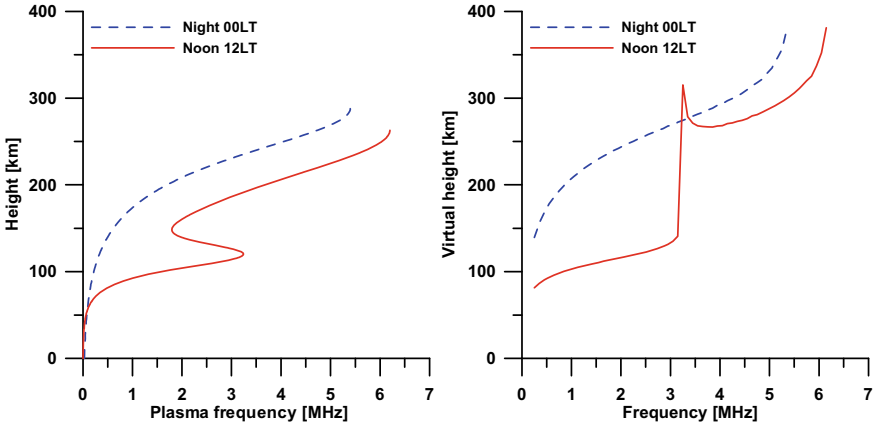

Fig. 7 (Left panel) model electron density profiles at noon (solid line) and midnight (dash line) conditions; (right panel) the corresponding model vertical ionograms

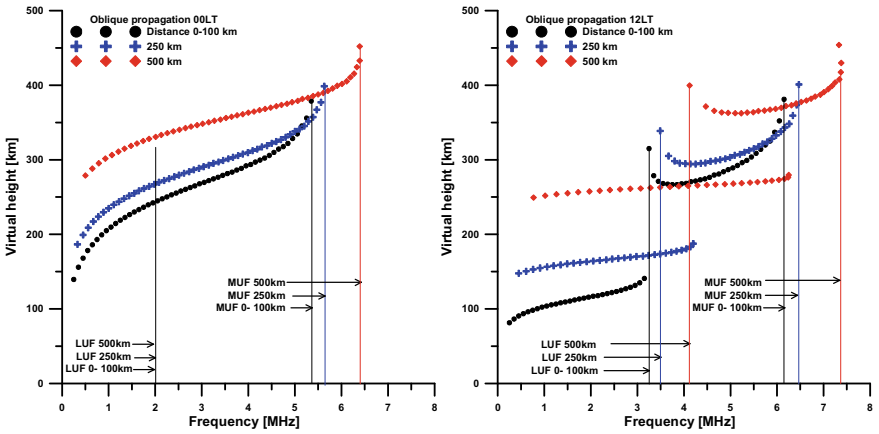

Fig. 8 Oblique ionograms based on the model profiles shown in the left panel of Fig. 7 at radio communication distances 0–100 km (dots), 250 km (crosses) *и* 500 km (diamonds) for midnight (left panel) and noon time (right panel) conditions

Figure 8 illustrates also the determination of the minimum and maximum usable frequencies at a given distance of the radio communication distance. At distances up to 100 km the reflection is practically vertical. The main condition is the reflection from the F region to be secured. The reflections from the E region (these are the frequencies lower than the area where the ionogram is interrupted, corresponding to *foE*) are practically not used due to the strong absorption of the radio waves.

Figure 9 presents the diurnal variability (LT dependence) of the calculated *LUF* (dash line) and *MUF* (solid line) for the considered in Fig. 8 three radio-path distances for a given date of 09 June 2014 according to the above presented methodology. At

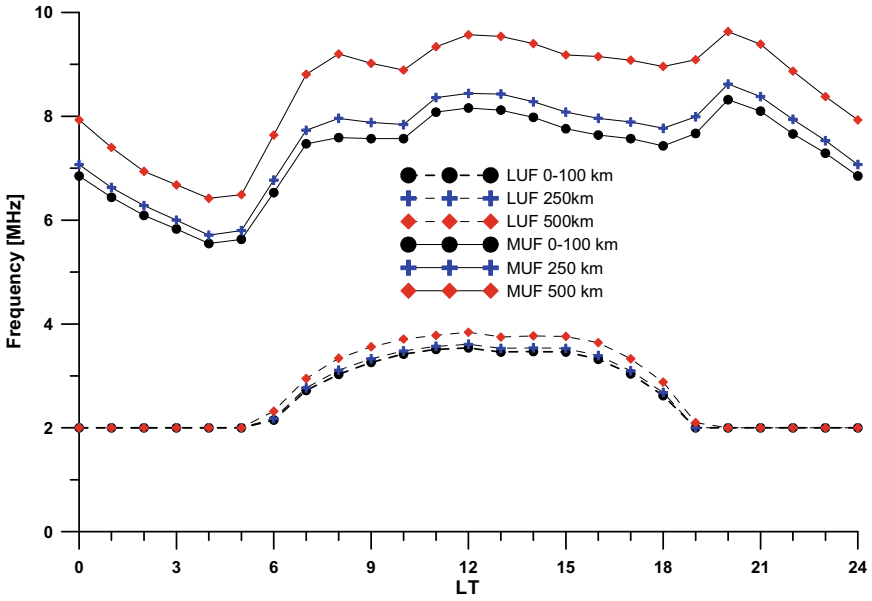

Fig. 9 Diurnal variability (LT dependence) of the *LUF* (dash line) and the *MUF* (solid line) calculated for three radio-path distances and for a given date of 09 June 2014

nigh conditions there is no *foE*, the electron density and respectively the radio wave absorption is low. Actually, the lowest usable frequency at night conditions is not determined by the state of the ionosphere but by technical considerations. Most of the shortwave transmitters have a frequency band from 1.5 to 30 MHz but the frequencies below 2 MHz fall within the field of broadcasting. Due to this reason the *LUF* at night conditions is accepted to be 2 MHz.

6 Conclusion

The methodology proposed in the present paper is intended for servicing users who carry out long-distance radio communications, as radio amateurs and government organizations. The methodology is suitable for organizing automatic data processing. In order to make a forecast for the propagation of radio waves at a given hour of the day, only three ionospheric characteristics are needed: *foE*, *foF2* and *MUF3000*. In the presence of working vertical ionosonde station the measured values of the above mentioned ionospheric characteristics can be used. A significantly new element of

this study is offering a methodology for forecasting the propagation of HF radio waves by reflection from the ionosphere over Bulgaria in a case when such equipment is absent. Then two types of new empirical models are provided: (i) for predicting *foE* that depends on the solar activity, and (ii) for estimating *foF2* and *MUF3000* based on the *TEC* data for the same or the closest point to already not working ionosonde station.

Summarizing it is worth noting that the presented new methodology for forecasting the propagation of HF radio waves by reflection from the ionosphere significantly increases the possibility for countries where the vertical sounding stations no longer operate. The International GNSS Service (IGS) has become a powerful *TEC* measurement tool to investigate the global and regional ionospheric structures owing to its continuous, easy operation, and worldwide distributed receivers. The IGS offers low cost information characterized by its accuracy, high temporal and spatial resolution, and availability.

Acknowledgements The present work is supported by the Bulgarian Ministry of Education and Science under the National Research Programme "Young scientists and postdoctoral students" approved by DCM № 577/ 17.08.2018. The presentation of the results is financed by Contract No D01-282/17.12.2019—Project "National Geoinformation Center (NGIC)" funded by the National Roadmap for Scientific Infrastructure 2017–2023 of Bulgaria.

References

1. Di Giovanni, G., Radicella, S.M.: An analytical model of the electron density profile in the ionosphere. Adv. Space Res. **10**(11), 27–30 (1990)
2. Barclay, L. (ed.): Propagation of Radio Waves. The Institution of Engineering and Technology, UK (2003)
3. Goodman, J.M.: Operational communication systems and relationships to the ionosphere and space weather. Adv. Space Res. **36**, 2241–2252 (2005)
4. Hanbaba, R.: Performance prediction methods of HF radio systems. Annali Di Geofis. **41**(5–6), 715–742 (1998)
5. Chapman, S.: The absorption and dissociative or ionizing effect of monochromatic radiation in an atmosphere on a rotating Earth. Proc. Phys. Soc. **43**, 26–45 (1931)
6. Pancheva, D., Mukhtarov, P.: A diurnal asymmetry of the monthly median E-region critical freouency. Adv. Space Res. **22**(6), 771–774 (1998)
7. Space Weather Prediction Center: https://www.swpc.noaa.gov/
8. Huang, J-.N.: The hysteresis variation of the semi-thickness of the F2-layer and its relevant phenomena at Kokubunji, Japan. J. Atmos. Terr. Phys. **25**, 647–658 (1969)
9. Gopal Rao, M.S.V., Sambasiva Rao, R.: The hysteresis variation in the F2-layer parameters. J. Atmos. Terr. Phys. **31**, 1119–1125 (1969)
10. Apostolov, E., Alberca, L., Pancheva, D.: Long-term prediction of the foF2 on the rising and falling parts of the solar cycle. Adv. Space Res. **14**(12), 47–50 (1994)
11. Pancheva, D., Mukhtarov, P.: A single-station spectral model of the monthly median F-region critical frequency. Annali Di Geofis. **39**(4), 807–818 (1996)
12. Mukhtarov, P., Pancheva, D., Andonov, B., Pashova, L.: Global TEC maps based on GNSS data: 1. Empirical background TEC model. J. Geophys. Res. Space Phys. **118**(7), 4594–4608 (2013)

13. Stankov, S.M., Jakowski, N., Heise, S., Muhtarov, P., Kutiev, I., Warnant, R.: A new method for reconstruction of the vertical electron density distribution in the upper ionosphere and plasmasphere. J. Geophys. Res. Space Phys. **108**(A5) (2003)
14. Pignalberi, A., Habarulema, J.B., Pezzopane, M., Rizzi, R.: On the development of a method for updating an empirical climatological ionospheric model by means of assimilated vTEC measurements from a GNSS receiver network. Space Weather **17**, 1131–1164 (2019)
15. Andonov, B.: Vertical total electron content and receiver bias calculations for Balkan Peninsula GNSS stations. C. R. Acad. Bulg. Sci. **70**(12), 1719–1729 (2017)
16. Dudeney, J.R., Kressman, R.I.: Empirical models of the electron concentration of the ionosphere and their value for radio communications purposes. Radio Sci. **21**(3), 319–330 (1986)
17. Cherny, F.B.: Radiowave propagation. M. Sov. Radio, 311–353 (in Russian) (1972)
18. Rawer, K.: Wave Propagation in the Ionosphere, vol. 5. Springer Science & Business Media (2013)